A Miniaturized Double-Surface CPW Bandpass Filter Improved Spurious Responses

Tatsuya Tsujiguchi, *Member, IEEE*, Haruo Matsumoto, *Member, IEEE*, and Toshio Nishikawa, *Fellow, IEEE*

***Abstract*—A novel miniaturized double-surface coplanar waveguide (CPW) filter has been developed. The filter is constructed by an electrode pattern of half-wavelength resonators on a double-sided circuit board with a high dielectric constant. A miniaturized pattern can be obtained by optimization of the electrode layout without any deterioration in unloaded Q. We use a particular pattern of via holes to reduce spurious responses. The filter is 38% smaller in size than the conventional $\lambda/4$ CPW filter. Spurious responses up to the third harmonic are suppressed by 13 dB, and satisfy the performance level required for industrial–scientific–medical band equipment. The measurement results agree well with the results of simulation.**

***Index Terms*—Coplanar waveguides, electric fields, finite-element method, microwave filters.**

I. Introduction

MINIATURIZATION of coplanar waveguide (CPW) filters [1]–[5] have been required for multichip modules.

The most general technique for miniaturization is to use $\lambda/4$ transmission-line resonators. CPW filters using $\lambda/4$ resonators are superior in terms of productivity because the shunt branch can be constructed in the uniplane [6]–[9]. However, there are limits to miniaturization of CPW filters because of the their low effective dielectric constant due to electromagnetic energy dissipation to an air field and their low unloaded Q due to the concentration of an electric field at the edges of the lines. As a solution to this problem, high-performance baluns and couplers using double-sided transmission lines and suspended strip-line filters using the double side of a substrate have been reported [10]–[13].

We propose high-performance CPW filters using an electromagnetic coupling by a electrode pattern on a double-sided metallized substrate with a high dielectric constant. We call these filters double-surface coplanar waveguide (DCPW) filters [14]. Each filter has a CPW interface and is easy to connect to a uniplanar circuit. Two different configurations are considered for DCPW filters (filters A and B), as shown in Fig. 1. In filter B, only the bottom surface electrode is shown. These filters are smaller in size and have higher unloaded Q compared with conventional $\lambda/4$ CPW filters. The resonant frequencies and their electromagnetic-field distributions for even and odd modes were calculated by a three-dimensional finite-element method (FEM), and the relationships between filter dimensions and parameters for filter design were obtained. The electrode pattern designs of the filters were also modified to suppress spurious responses. We call these filters modified filters as compared with original filters. Consequently, the spurious responses satisfy the required characteristics for practical use, such as use in industrial–scientific–medical (ISM) equipment.

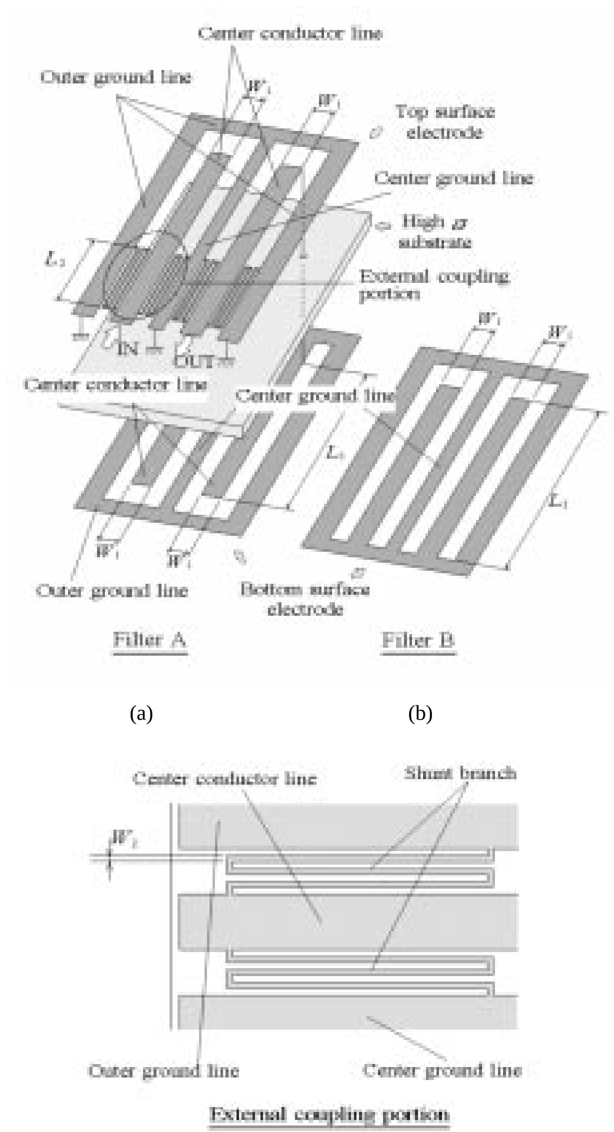

Fig. 1. Construction of the filters. (a) Filter A. (b) Filter B. (c) Enlargement of the external coupling portion.

Manuscript received March 31, 2000; revised July 31, 2000.

T. Tsujiguchi and H. Matsumoto are with the Kanazawa Murata Manufacturing Company Ltd., Ishikawa 921-2101, Japan.

T. Nishikawa is with the Cooperative Research Center, Saitama University, Saitama 331-0852, Japan.

Publisher Item Identifier S 0018-9480(01)03303-8.

In this paper, we mainly discuss filter A and describe its construction, an equivalent circuit and simulation, and performances of trial filters.

II. Construction

Construction of a DCPW filter chip (filter A) is shown in Fig. 1(a) and another construction (filter B) is shown in Fig. 1(b). The filters are constructed by electrode patterns on a double-sided ceramic substrate with a high dielectric constant $(\varepsilon_r = 39)$ [15]. The electrode pattern on the bottom surface in the case of filter B is the inverse of that in the case of filter A.

The electrodes on the top and bottom surfaces of the substrate are each patterned as two center conductor lines, a center ground line, and outer ground lines. Every center conductor line has an open end, and two center conductor lines are arranged in parallel on each plane of the substrate.

The opposite facing center conductor lines of the top and bottom surfaces function as a balanced resonator, and the overlap lengths of the lines (L_1) on the top and bottom surfaces determine the resonant frequency. Two resonators are electromagnetically coupled to each other, and the widths of the lines (W_1) determine the bandwidth of the filter.

I/O ports are extracted from the center conductor lines on the top surface, and the ports are isolated by the center ground line between them. An external Q is inductively obtained by a shunt branch of a meandering configuration that connects between the center conductor line and the ground line near the I/O ports on the top surface. The length of the shunt branch (L_2) determines the external Q.

The substrate with a high dielectric constant is metallized with three metal layers. Ti and Pd layers are formed by evaporation, and then an Au layer of about 5 μm in thickness is formed by electrical plating. The electrode pattern is transcribed by photolithography. The narrowest width of the line is 30 μm, and the tolerance is within 8 μm.

The filter is suitable for flip-chip mounting on a circuit board and for multichip modules. The variation of the center frequency by mounting on a circuit board is one-third of that of a conventional $\lambda/4$ CPW filter under the same mounting conditions because the electromagnetic energy is fully confined in the high dielectric-constant substrate.

III. Equivalent Circuit and Design

A. Equivalent Circuit

An equivalent circuit of filter A is shown in Fig. 2. The values of elements are shown in Table I, in the case of $L_1 = 3.0$ mm, $W_1 = 0.3$ mm, and $L_2 = 1.5$ mm.

The center conductor lines consist of two sections (Z_1, Z_8), the outer ground line consists of five sections $(Z_5, Z_4, Z_5', Z_7, Z_6)$, and the center ground lines consist of three sections (Z_3, Z_2, Z_3'). Fringing capacitors (c_1, c_2) and the inductors $(\boldsymbol{l}_1, \boldsymbol{l}_2)$ are added in the discontinuities parts of the transmission lines. The shunt branches of meandering configuration are represented by the lumped element circuits, inductors $(\boldsymbol{l}_{3\text{-}6})$, and capacitors (c_{3-5}). The characteristic impedance (Z_n) and the propagation constant $(\alpha + j\beta)$ of each line are obtained by calculation of propagation modes in a two-dimensional waveguide by the FEM. Each lumped element value is obtained by the FEM using a three-dimensional model.

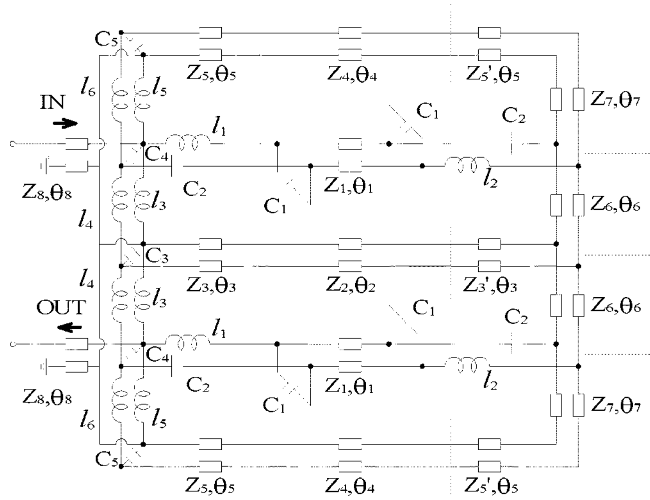

Fig. 2. Equivalent circuit of the filter (filter A).

TABLE I
VALUES OF ELEMENTS OF THE EQUIVALENT CIRCUIT

Characteristic impedance Zn (Ω)		α (dB/m) 2.4GHz	β (rad/m) 2.4GHz	Length (mm)
Z_1	25.66	4.43	285.64	3.0
Z_2	33.16	5.06	286.78	3.0
Z_3	66.17	2.71	267.36	0.75
Z_3'	36.83	4.79	287.06	0.75
Z_4	27.43	4.49	266.79	3.0
Z_5	38.72	2.93	261.04	0.75
Z_5'	28.72	4.38	268.04	0.75
Z_6	25.89	4.85	287.47	0.65
Z_7	25.89	4.85	287.47	0.55
Z_8	27.14	3.85	273.94	0.3

Capacitance (pF)	
C_1	0.082
C_2	0.011
C_3	0.207
C_4	0.311
C_5	0.155

Inductance (nH)	
$\boldsymbol{l}_1$	0.18
$\boldsymbol{l}_2$	0.18
$\boldsymbol{l}_3$	2.436
$\boldsymbol{l}_4$	0.104
$\boldsymbol{l}_5$	2.436
$\boldsymbol{l}_6$	0.104

Filter dimensions

Dimensions	W	D	T	W_1	W_2	L_1	L_2
(mm)	5.2	2.5	0.2	0.3	0.03	3.0	1.5

B. DCPW Modes

The filter has coupling by the odd and even modes. The electric-field distributions of the dominant modes are shown in Fig. 3, where the shunt branch is simplified to eliminate the influence of external coupling.

In the odd mode, the electric-field lines of the first and second resonators extend in inverse directions, as shown in Fig. 3(a). An electric wall exists in the middle of the center ground line. The surface current of the first resonator flows into the second resonator through the outer ground line.

In the even mode, the electric-field lines of the first and second resonators extend in the same directions, as shown in Fig. 3(b). A magnetic wall exists in the middle of the center ground line. The surface current of the first resonator flows into the outer ground line and does not flow into the second resonator.

Consequently, the center conductor lines and outer ground line function as a $\lambda/2$ resonator like a hairpin resonator.

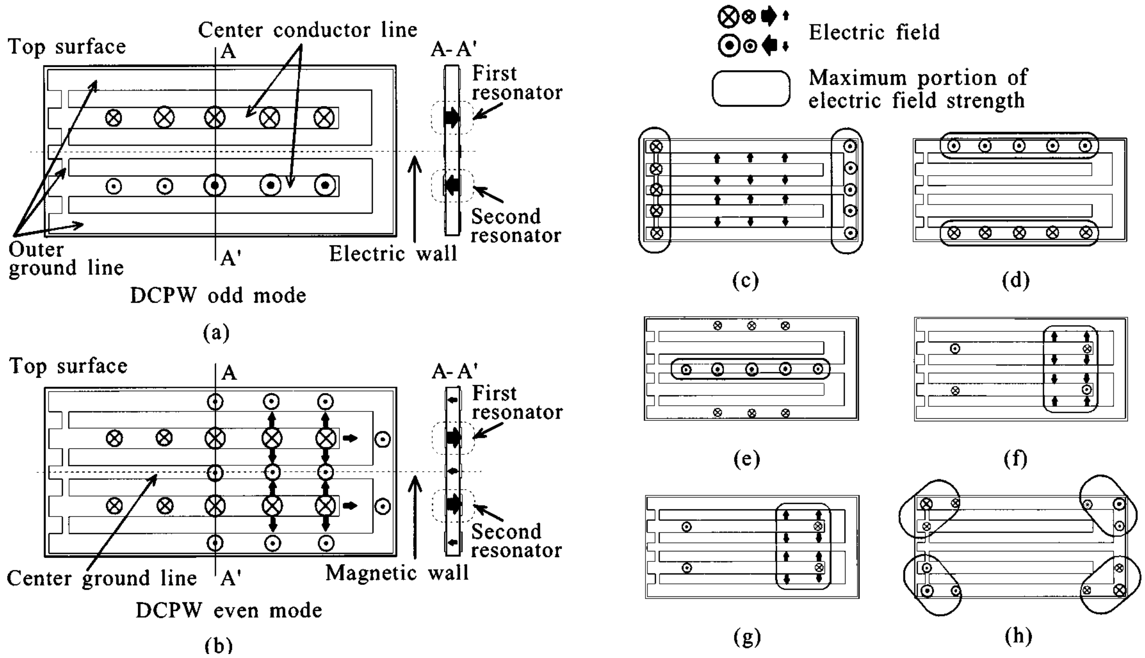

Fig. 3. Electric-field distributions of the filter (filter A). (a) DCPW odd mode. (b) DCPW even mode. (c)–(h) Spurious responses. The strength of the electric field is expressed by the sizes of the arrows and symbols.

TABLE II
COMPARISON OF THE FILTER AND CONVENTIONAL $\lambda/4$ CPW FILTER

Filter type	Mode	$f$even , $f$odd (MHz)	Center frequency(MHz)	Qeven Q odd	Average Q	Unloaded Q	Size(mm ^{3}) (V)
DCPW	Odd	2312.76	2479.42	61.06	61.32	73.14	5.2×2.5×0.2
	Even	2646.07	($f$even+$f$odd)/2	61.58	(Qeven+Qodd)/2		(2.60)
CPW	Even	2500.68	2586.19	53.94	55.15	70.38	8.4×2.5×0.2
	Odd	2671.70	($f$even+$f$odd)/2	56.36	(Qeven+Qodd)/2		(4.20)

TABLE III
CALCULATED RESONANT FREQUENCIES OF THE FILTERS

Filter type	Frequency of the modes (GHz)							
	(a)	(b)	(c)	(d)	(e)	(f)	(g)	(h)
Filter A	2.30	2.69	4.04	4.36	5.61	5.71	5.77	7.84
Filter B	3.08	3.10	4.95	4.53	5.71	4.91	4.67	7.82

The center frequency and unloaded Q are shown in Table II, where the DCPW filter and the conventional $\lambda/4$ CPW filter are measured at the same coupling levels. The size of the filter is 38% smaller and the unloaded Q is higher than those of the conventional filter.

Miniaturization is achieved because a high dielectric-constant material contributes to concentrate the electric field into the substrate, an outer ground line is used as a portion of the resonator, and the Q value is maintained due to mitigation of the edge effect of the electric field in the lines.

C. Spurious Responses

The DCPW filters have several higher order modes in addition to the above-mentioned odd and even modes. The electric-field distributions of these modes are shown in Fig. 3(c)–(h), and the resonant frequencies calculated by the three-dimensional FEM for filter A are shown in Table III. The transmission characteristics of the filter (filter A) in a weak external coupling condition are shown in Fig. 4. There are six spurious responses up to 8 GHz, where these responses correspond to the electric-field distribution shown in Fig. 3(c)–(h) . The measured frequencies of higher order modes agree with the calculated frequencies within $\pm 2\%$.

The spurious responses that have the electric field distributions shown in Fig. 3(c), (d), and (h) depend mainly on the filter shape. The spurious response that has the electric-field distribution shown in Fig. 3(e) depends on the shape of the center ground line. In order to use the filter for specific applications, it is necessary to suppress these spurious responses close to $2F_0$ (4.8 GHz) and $3F_0$ (7.2 GHz).

The filters have spurious responses, as shown in the Fig. 3(f) and (g), which indicate similar electric-field distributions as those of the $\lambda/4$ CPW filter. These resonant frequencies are 5.71 and 5.77 GHz in filter A and 4.91 and 4.67 GHz in filter B. The resonant frequencies in filter A become higher than those in filter B because of the influence of the bottom surface electrode. Consequently, filter A is superior in spurious response near $2F_0$ of the filter in comparison with filter B.

D. Physical Parameters

1) Center Frequency and the Coupling Coefficient: The relationship between the center frequency of the filter (F_0) and L_1 is shown in Fig. 5. The center frequency can be controlled by the

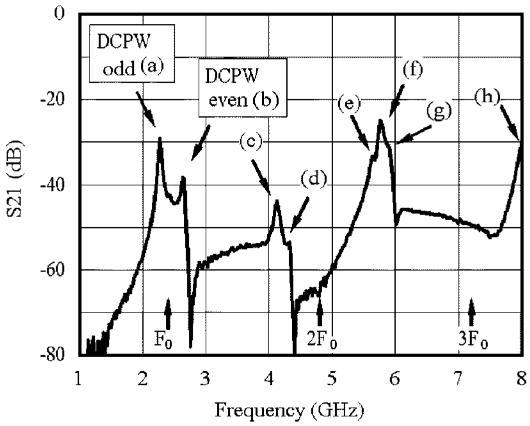

Fig. 4. Transmission characteristics of the filter (filter A).

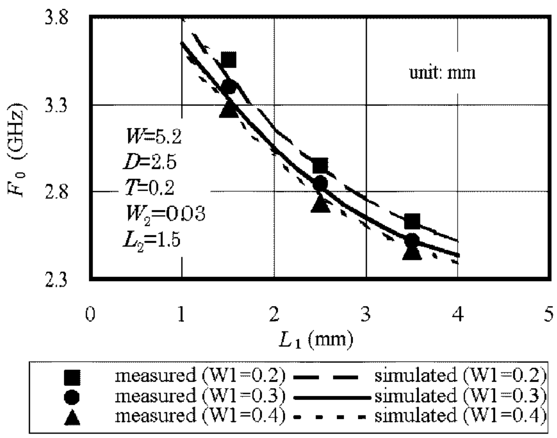

Fig. 5. Center frequency (F_0) versus $L1$.

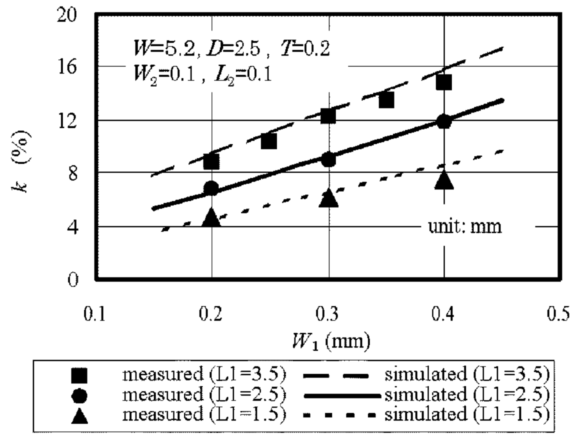

Fig. 6. Coupling coefficient (k) versus $W1$.

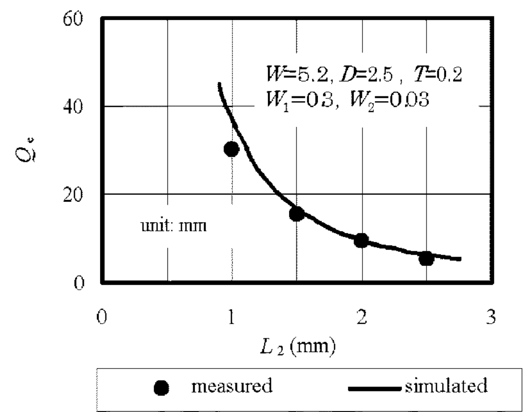

Fig. 7. External Q (Qe) versus $L2$.

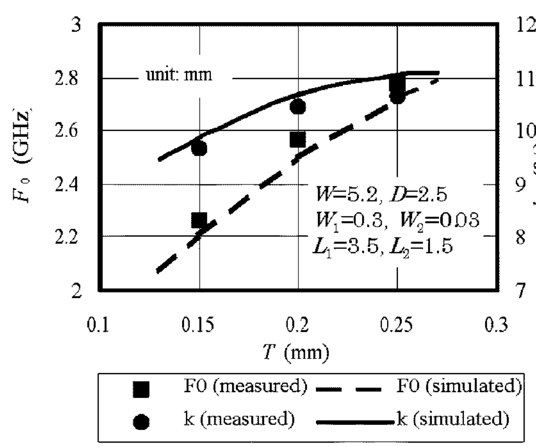

Fig. 8. Center frequency (F_0) and coupling coefficient (k) versus T.

L_1 value. The relationship between the coupling coefficient (k) and W_1 is shown in Fig. 6. The resonant frequency of the even mode (f_{even}) and that of the odd mode (f_{odd}) were calculated by the FEM and were measured using a weak external-coupling sample. In this sample, the shunt brunch is not a meandering line, but a straight line ($W_2 = 0.1$ mm, $L_2 = 0.1$ mm). The coupling coefficient is proportional to the W_1 values, and it is considerably dependent on the L_1 values.

2) Unloaded Q (Q_0): The unloaded Q (Q_0) values of the resonator and the conventional $\lambda/4$ CPW resonator were measured using a weak external coupling model. The results of measurements are shown in Table II. The Q_0 value of the resonator is 3.9% higher than that of the conventional $\lambda/4$ CPW resonator.

The insertion loss of the filter was calculated using the attenuation constant, which was obtained by the calculation of propagation modes in a two-dimensional waveguide by the FEM.

3) External Q (Q_e): A resonator is connected to an external circuit through the CPW line (Z_8) and the inductor $(\boldsymbol{l}_3)$ of a meandering line. The relationship between the external Q (Q_e) of the filters and L_2 is shown in Fig. 7. The Q_e value varies according to the L_2 value and the configuration of the meandering line.

4) Influence of the Substrate Thickness: In the case of DCPW filters, the filter characteristics are considerably influenced by chip thickness because of the electrode pattern on both surface. The relationships between F_0, k, and chip thickness (T) are shown in Fig. 8. The thickness variation is controlled within 5 μm, and the frequency and coupling variations are, therefore, controlled within 25 MHz and 0.05%, respectively. These simulation data were also obtained by the FEM and were confirmed by measurements. The values of F_0, k, Q_0 and Q_e

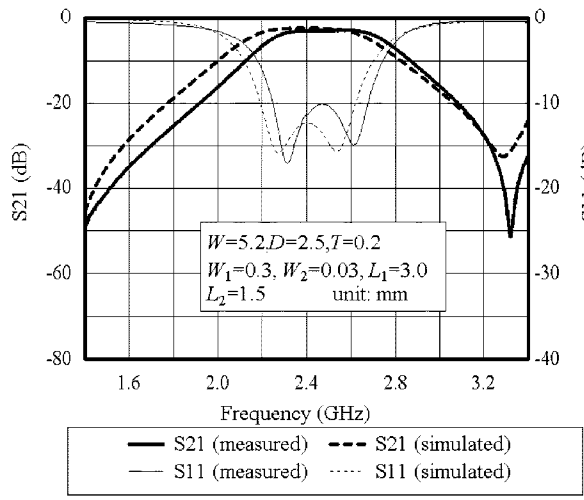

Fig. 9. Transmission and return-loss characteristics.

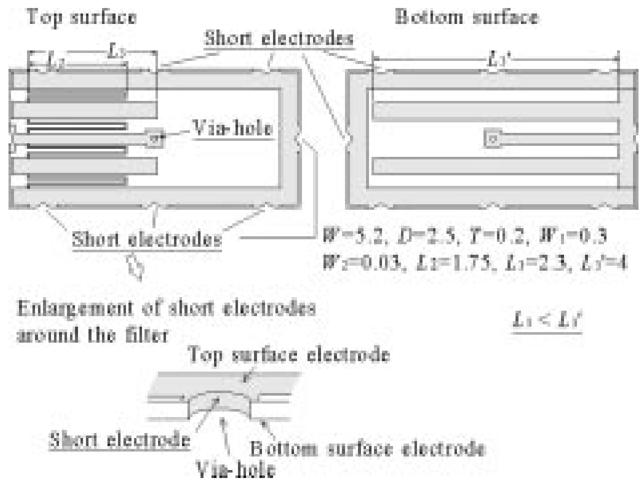

Fig. 10. Two-section filter. Bottom surface is drawn perspectively.

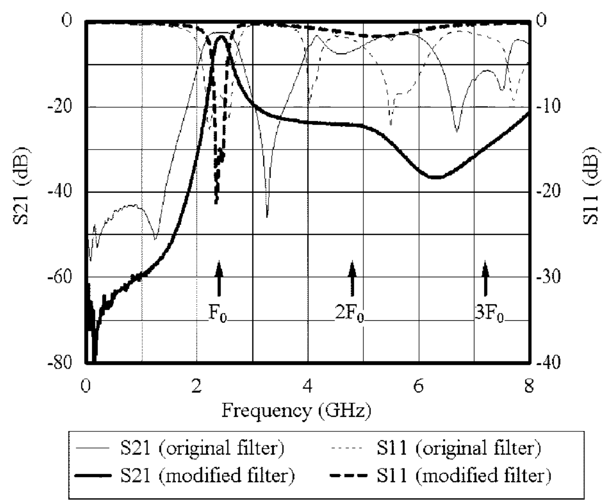

Fig. 11. Transmission and return-loss characteristics (original and modified two-section filters).

were predetermined by the required characteristics, and the physical parameters of the filter chip were determined by each of the relationships shown in Figs. 5–8.

IV. Experimental Results

A. Characteristics of DCPW Filter

A two-section filter (filter A) with a center frequency of 2.4 GHz and a bandwidth of 400 MHz was designed and made. The minimum insertion loss of the trial filter is 2.89 dB at 2.49 GHz and the chip size is $5.2 \times 2.5 \times 0.2$ mm^3. The dimensions are $L_1 = 3.0$ mm, $W_1 = 0.3$ mm, and $L_2 = 1.5$ mm. This filter is 38% smaller in size than the conventional $\lambda/4$ CPW filter. The external coupling is optimized by the meandering line length (L_2). The measured and simulated transmission and return-loss characteristics are shown in Fig. 9. The measurement results agree well with the simulation results.

Next, a filter (filter B) with a center frequency of 2.4 GHz and a bandwidth of 400 MHz was designed and made. The minimum insertion loss at 2.42 GHz is 2.58 dB ($5.2 \times 2.5 \times 0.2$ mm^3). The dimensions are $L_1 = 3.5$ mm, $W_1 = 0.3$ mm, and $L_2 = 1.5$ mm. The same center frequency as that in filter B is realized in filter A by a shorter center conductor line length. Thus, a smaller size can be achieved by the use of filter A than by the use of filter B. The reason for this is that the electric-field distribution at the open end of both surfaces acts to negate each other in filter B.

B. Spurious-Suppressed DCPW Filters

The spurious suppression method is discussed for two- and three-section filters.

The two-section filter design (filter A) was modified to suppress spurious responses. The design of the two-section filter is shown in Fig. 10.

The short electrodes that connect the top surface to the bottom surface by via holes suppress the spurious responses that arise from the filter shape. There are six short electrodes on the long sides of the filter chip. These electrodes suppress the spurious response that corresponds to the electric-field distribution shown in Fig. 3(d). There are also two short electrodes on the short sides of the filter chip. These electrodes suppress the spurious responses that correspond to the electric-field distributions shown in Fig. 3(c) and (h).

The via hole located at the center of the filter suppresses the spurious responses that arise from the center ground line [see Fig. 3(e)]. These via holes were made by laser drilling, and it is possible to make holes of 100 μm in size.

The center conductor lines on the top surface are shortened and those on the bottom surface are lengthened $(L_3 < L_3')$. Consequently, the frequencies of spurious responses that have the electric-field distributions shown in Fig. 3(f) and (g) become sufficiently high without changing the resonant frequencies of the dominant modes because these responses are mainly dependent on the top surface, and the dominant modes are dependent on both surfaces.

The measured transmission and return-loss characteristics of the modified filter and the original filter (mentioned in Section IV-A) are shown in Fig. 11. The insertion loss of the two-section filter is 3.58 dB at 2.42 GHz, and the attenuations of

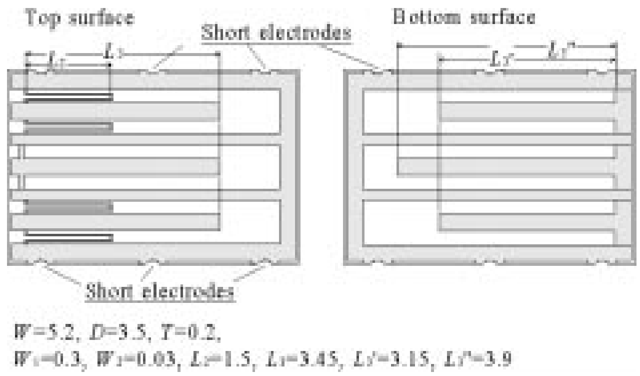

Fig. 12. Three-section filter. Bottom surface is drawn perspectively.

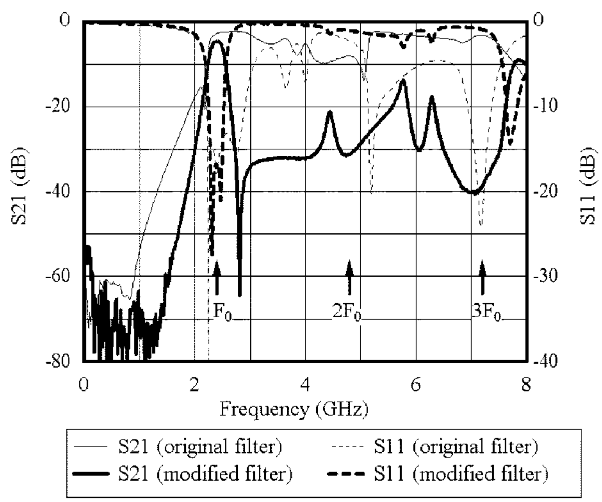

Fig. 13. Transmission and return-loss characteristics (original and modified three-section filters).

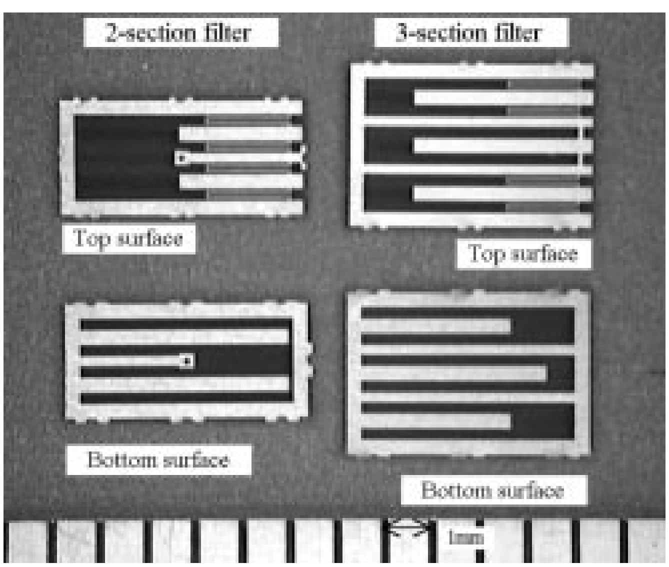

Fig. 14. Two and three-section filters.

$2F_0$ and $3F_0$ are 24.2 and 29.6 dB, respectively. The resonant frequency of the even mode becomes lower because of the short electrodes by the via holes. Therefore, the bandwidth of the filter becomes narrower than that of the original filter.

We designed experimental three-section filters that have electrode patterns on both planes like the two-section filters. Generally, attenuation characteristics can be improved by increasing the number of sections. However, in the case of a three-section filter, in which spurious responses are not suppressed (original), the attenuation characteristics in fact deteriorate because many of the spurious responses appear at a frequency slightly higher than the passband of the filter. The three-section filter was, therefore, modified to suppress the spurious response by the same method as that used for the two-section filter. The design of the three-section filter is shown in Fig. 12. The measured transmission and return-loss characteristics of the filter and original filter are shown in Fig. 13. The short electrodes and center conductor line configuration sufficiently suppress the spurious responses. The insertion loss of the three-section filter is 4.67 dB at 2.39 GHz, and the chip size is 5.2 × 3.5 × 0.2 mm^3. The attenuations of $2F_0$ and $3F_0$ are 31.2 and 38.4 dB, respectively. These filters are useful for various applications.

A photograph of two- and three-section filters is shown in Fig. 14. In the filter, via holes are arranged around the filter chip.

V. Conclusion

Novel high-performance CPW filters using both sides of a substrate have been developed. The filter is constructed by an electrode pattern of half-wavelength resonators on a double-sided circuit board with a high dielectric constant. The electromagnetic-field distribution and the electromagnetic coupling were analyzed, and the equivalent circuit and filter design parameters were then obtained. Two- and three-section trial filters were designed and made. The measurement results agreed well with the results of simulation. The two-section trial filter was 38% smaller in size than the conventional $\lambda/4$ CPW filter without any deterioration in unloaded Q. This filter has a bandwidth of 400 MHz at 2.49 GHz with an insertion loss of 2.89 dB, and the chip size is 5.2 × 2.5 × 0.2 mm^3 (filter A).

We used a particular pattern of via holes to reduce spurious responses. Consequently, the attenuations of $2F_0$ and $3F_0$ are more than 20 dB in the two-section filter and 30 dB in the three-section filter, and satisfy the performance level required for ISM band equipment. Moreover, it is easy to mount as a chip in the uniplanar circuits by a CPW interface.

Acknowledgment

The authors would like to thank Prof. T. Hata, Kanazawa University, Ishikawa, Japan, and Assoc. Prof. K. Sasaki, Kanazawa University, Ishikawa, Japan, for their support and guidance throughout the course of this study. The authors would also like to thank K. Matsunaga, Kanazawa Murata Manufacturing Company Ltd., Ishikawa, Japan, for his support during the preparation of this paper.

References

[1] K. C. Gupta, R. Garg, I. Bahl, and P. Bhartia, *Microstrip Lines and Slotlines*, 2nd ed. Norwood, MA: Artech House, 1996.

[2] D. F. Williams and S. E. Schwarz, "Design and performance of coplanar waveguide bandpass filters," *IEEE Trans. Microwave Theory Tech.*, vol. MTT-31, pp. 558–566, July 1983.

[3] W. Menzel, W. Schwab, and G. Strauss, "Investigation of coupling structure for coplanar filter," in *IEEE MTT-S Int. Symp. Dig.*, Orlando, FL, May 1995, pp. 1407–1410.

[4] F. L. Lin, C. W. Chiu, and R. B. Wu, "Coplanar waveguide bandpass filter—A ribbon-of-brick-wall design," *IEEE Trans. Microwave Theory Tech.*, vol. 43, pp. 1589–1596, July 1995.

[5] J. K. A. Everard and K. K. M. Cheng, "High-performance direct coupled bandpass filter on coplanar waveguide," *IEEE Trans. Microwave Theory Tech.*, vol. 41, pp. 1568–1573, Sept. 1993.

[6] K. Silvanand, S. Uysal, and K. W. Eccleston, "CPW bandpass filters using end-coupled quarter-wavelength resonators," *Microwave Opt. Technol. Lett.*, vol. 15, pp. 29–33, May 1997.

[7] T. Tsujiguchi, H. Matsumoto, and T. Nishikawa, "A miniaturized end-coupled bandpass filter using $\lambda/4$ hair-pin coplanar resonators," in *IEEE MTT-S Int. Microwave Symp. Dig.*, Baltimore, MD, June 1998, pp. 829–832.

[8] Y. Noguchi, J. Ishii, H. Miyake, and Y. Takeda, "A novel method of spurious suppression of bandpass filter using coplanar waveguide resonators," in *Proc. URSI ISSSE Symp. Dig.*, Sept. 1992, pp. 867–870.

[9] K. Hettak, J. P. Coupez, E. Rius, and Toutain, "A new uniplanar bandpass filter using $\lambda g/2$ slotline and $\lambda g/4$ coplanar waveguide resonators," in *Proc. 24th European Microwave Conf.*, Cannes, France, Sept. 1994, pp. 1360–1366.

[10] M. Aikawa and H. Ogawa, "Double-sided MIC's and their applications," *IEEE Trans. Microwave Theory Tech.*, vol. 37, pp. 406–413, Feb. 1989.

[11] W. Schwab and W. Menzel, "Compact bandpass filter with improved stopband characteristics using planar multilayer structures," in *IEEE MTT-S Int. Microwave Symp. Dig.*, Albuquerque, NM, June 1992, pp. 1207–1209.

[12] W. Schwab, F. Boegelsack, and W. Menzel, "Multilayer suspended stripline and coplanar line filters," *IEEE Trans. Microwave Theory Tech.*, vol. 42, pp. 1403–1407, July 1994.

[13] C. Nguyen, "Unsymmetrical broadside-coupled coplanar waveguides for loose- and tight-coupling MIC and MMIC applications," *Int. J. Infrared Millim. Waves*, vol. 17, pp. 1321–1326, Aug. 1996.

[14] T. Tsujiguchi, H. Matsumoto, and T. Nishikawa, "A miniaturized bandpass filter with double surface," in *IEEE MTT-S Int. Microwave Symp. Dig.*, Boston, MA, June 2000, pp. 199–202.

[15] K. Wakino, T. Nishikawa, S. Tamura, and Y. Ishikawa, "Microwave bandpass filters containing dielectric resonators with improved temperature stability and spurious response," *IEEE MTT-S IEEE Catalog*, no. 75, CH095-65, pp. 63–65, May 1975.

Tatsuya Tsujiguchi (M'98) was born in Ishikawa, Japan, on September 13, 1965. He received the B.E. and M.E. degrees in electronics and computer science from Kanazawa University, Ishikawa, Japan, in 1988 and 1990, respectively, and is currently working toward a graduate degree at Kanazawa University.

In 1990, he joined the Kanazawa Murata Manufacturing Company Ltd., Ishikawa, Japan. He is currently with the Graduate School of Natural Science and Technology, Kanazawa University, where he is engaged in the design of a dielectric filter.

Mr. Tsujiguchi is a member of the Institute of Electronics, Information and Communication Engineers (IEICE), Japan.

Haruo Matsumoto (M'91) was born in Ishikawa, Japan, on October 27, 1948. He received the B.E. and M.E. degrees in electrical engineering from Ritsumeikan University, Kyoto, Japan, in 1971 and 1973, respectively, and the Doctor of Engineering degree from Kanazawa University, Ishikawa, Japan, in 1993.

In 1973, he joined the Murata Manufacturing Company Ltd., Kyoto, Japan. In 1985, he transferred to the Kanazawa Murata Manufacturing Company Ltd., Ishikawagun Ishikawa, Japan, where he is currently a Director engaged in the design of dielectric filters.

Dr. Matsumoto is a member of the Institute of Electronics, Information and Communication Engineers (IEICE), Japan.

Toshio Nishikawa (M'86–SM'90–F'97) was born in Ishikawa, Japan, on July 10, 1935. He received the B.E. degree in electrical engineering and the Doctor of Engineering degree from Kanazawa University, Ishikawa, Japan, in 1958 and 1990, respectively.

In 1961, he joined the Murata Manufacturing Company Ltd., Kyoto, Japan. He is currently a Guest Professor with the Cooperative Research Center, Saitama University, Saitama, Japan. His research activities are mainly concerned with dielectric resonators and their application to microwave components.

Dr. Nishikawa is a member of the Institute of Electronics, Information and Communication Engineers (IEICE), Japan, and the Information Processing Society (IPSJ), Japan.